Mössbauer Spectroscopy of Mixed-Valence Biferrocenes in High Magnetic Fields

Michelle J. Cohn, Mark D. Timken, and David N. Hendrickson*

Contribution from the School of Chemical Sciences, University of Illinois, Urbana, Illinois 61801. *Received January 9, 1984*

Abstract: The Mössbauer technique is employed to investigate the electronic structure of salts of various mixed-valence biferrocenium and mononuclear ferrocenium cations in high magnetic fields. The internal magnetic field at the iron nucleus is gauged with the magnetic Mössbauer technique to characterize the unpaired-electron orbital. The effective magnetic field at the iron nucleus in a series of four substituted ferrocenium cations (PF_6^- salts) was found to vary considerably. This, together with the observation of pronounced temperature dependence in the Mössbauer spectrum of ferrocenium hexafluorophosphate in a 60-kG external field, indicates the presence of spin–lattice relaxation effects. The electron spin relaxation rate is greater than the ^{57}Fe nuclear Larmor precession frequency for decamethylferrocenium hexafluorophosphate at 5 K. The presence of such electron spin relaxation effects was verified for biferrocenium triiodide by observing the Mössbauer spectrum of this mixed-valence species as a function of temperature in a 55-kG external field. The establishment that spin relaxation affects the magnitude of the internal magnetic field at the iron nucleus invalidates a previous suggestion that the small internal field at the iron(III) ion in the mixed-valence biferrocene cation results from the fact that the unpaired electron resides in an orbital of predominantly ligand character. Finally, Mössbauer spectra were obtained at fields of 30, 51, and 60 kG for the Mössbauer-delocalized triiodide salts of mixed-valence bis(fulvalene)diiron and [2.2]ferrocenophane-1,13-diyne monocations. These Mössbauer spectra were simulated with an $S = {}^1/_2$ spin Hamiltonian computer program to give estimates of the components of the hyperfine interaction tensor.

The study of binuclear mixed-valence transition-metal complexes is proving to be useful in characterizing the factors controlling electron transfer between transition-metal ions.[1,2] By employing the intrinsic time scales associated with various spectroscopic techniques, it has been possible to bracket the electron-transfer rates for a number of mixed-valence biferrocenes.[3,4] Until very recently only two types of mixed-valence biferrocenes have been noted. There are those that have been characterized to have distinguishable Fe(II) and Fe(III) sites on the ^{57}Fe Mössbauer time scale, which means that the electron-transfer rate is less than $\sim 10^7$ s^{-1}. On the other hand, several mixed-valence biferrocenes have been shown to have indistinguishable iron sites (i.e., "average valence") on the Mössbauer and EPR time scales, which means that the electron-transfer rate is greater than 10^{11} s^{-1}. In fact, it appears that the ground state of this latter type of mixed-valence biferrocene is completely delocalized with two equivalent iron ions.[5] There is no potential energy barrier present in the ground state in spite of the fact that the iron ions are well separated in many of these species as exemplified by the mixed-valence complex I, the [2.2]-ferrocenophane-1,13-diyne cation. Very recently Sano et al.[6,7]

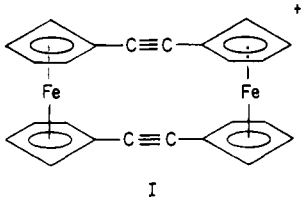

I

described three mixed-valence biferrocenes that interconvert more rapidly than the Mössbauer time scale at room temperature (one quadrupole-split doublet), but upon cooling to liquid-nitrogen temperature, each of the complexes interconverts more slowly than Mössbauer time scale.

A detailed explanation for why electron transfer is so rapid in certain mixed-valence biferrocenes, whereas it is so slow in others, has not been advanced. The PKS vibronic model[8] would say that there are three factors: (1) the electronic coupling between the orbitals on the two iron centers, (2) the zero-point energy difference between the orbitals on the two ferrocenyl moieties in a binuclear complex, and (3) the magnitude of vibronic coupling in a mixed-valence biferrocene. The PKS vibronic model obviously considers only the isolated molecule (cation). It is quite possible that transformations seen for mixed-valence complexes in the solid state are cooperative. Spin-crossover[9,10] and Jahn–Teller[11] interacting complexes are two other examples of energetically labile[12] species which have been demonstrated to undergo cooperative transformations in the solid state (phase transitions).

Kirchner et al.[13] in 1976 reported the results of iterative extended-Hückel molecular orbital calculations for biferrocene and various oxidation states of bis(fulvalene)diiron. For biferrocene it was found that there can be appreciable mixing between the highest energy π-orbitals of the fulvalenide ligand and the iron d-orbitals. It was quite reasonable then that Frankel et al.[14] turned to the Mössbauer technique to determine the nature of the magnetic hyperfine field at the Fe(II) and Fe(III) centers in magnetically perturbed mixed-valence biferrocene(1+). They concluded that the unpaired electron in this cation "occupies a predominantly ligand-based orbital which is asymmetric with respect to the two iron sites". Soon after this, a detailed Mössbauer study of mixed-valence biferrocenes in high magnetic fields was initiated in our laboratories, the results of which are presented in this paper.

(1) "Mixed-Valence Compounds, Theory and Applications in Chemistry, Physics, Geology, and Biology"; Brown, D. B., Ed.; Reidel Publishing Co.: Boston, 1980.
(2) Day, P. *Int. Rev. Phys. Chem.* **1981**, *1*, 149.
(3) Morrison, W. H., Jr.; Hendrickson, D. N. *Inorg. Chem.* **1975**, *14*, 2331.
(4) Le Vanda, C.; Bechgaard, K.; Cowan, D. O.; Mueller-Westerhoff, U. T.; Eilbracht, P.; Candela, G. A.; Collins, R. L. *J. Am. Chem. Soc.* **1976**, *98*, 3181.
(5) Kramer, J. A.; Hendrickson, D. N. *Inorg. Chem.* **1980**, *19*, 3330.
(6) Iijima, S.; Motoyama, I.; Sano, H. *Bull. Chem. Soc. Jpn.* **1980**, *53*, 3180.
(7) Iijima, S.; Saida, R.; Motoyama, I.; Sano, H. *Bull. Chem. Soc. Jpn.* **1981**, *54*, 1375.
(8) Wong, K. Y.; Schatz, P. N. *Prog. Inorg. Chem.* **1981**, *28*, 369.
(9) Haddad, M. S.; Lynch, M. W.; Federer, W. D.; Hendrickson, D. N. *Inorg. Chem.* **1981**, *20*, 123; *Ibid.* **1981**, *20*, 131.
(10) Gütlich, P. *Struct. Bonding (Berlin)* **1981**, *44*, 83.
(11) Reinen, D.; Friebel, C. *Struct. Bonding (Berlin)* **1979**, *37*, 1.
(12) Ammeter, J. H. *Nouv. J. Chim.* **1980**, *4*, 631. Ammeter, J. H.; Zoller, L.; Bachmann, J.; Baltzer, E.; Gamp, E.; Bucher, R.; Deiss, E. *Helv. Chim. Acta* **1981**, *64*, 1063.
(13) Kirchner, R. F.; Loew, G. H.; Mueller-Westerhoff, U. T. *Inorg. Chem.* **1976**, *15*, 2665.
(14) Rudie, A. W.; Davison, A.; Frankel, R. B. *J. Am. Chem. Soc.* **1979**, *101*, 1629.

0002-7863/84/1506-6683$01.50/0

Theoretical Background

The ^{57}Fe nucleus has a nuclear ground state with $I = {}^1/_2$ and an excited nuclear state with $I = {}^3/_2$. For many iron compounds, the nuclear excited state is split into two levels due to an electric quadrupole interaction (ΔE_Q) between the quadrupole moment of the nucleus and the electric field gradient (i.e., asymmetry in electron distribution) at the nucleus. The introduction of an external magnetic field leads to the Zeeman splitting of the ^{57}Fe ground and excited states.[15] In the present paper, polycrystalline samples are employed, and the experimental spectrum is a superposition of many spectra determined by the various orientations of the hyperfine and/or electric field gradient tensors with both the γ-ray propagation vector and the external magnetic field direction.

In this paper, paramagnetic species which have an $S = {}^1/_2$ ground state well-separated from other electronic states were studied by applying a large, external magnetic field parallel to the γ-ray beam. The spin Hamiltonian for such an $S = {}^1/_2$ species is given as

$$\hat{\mathcal{H}} = \beta_e \hat{S}\cdot\mathbf{g}\cdot\hat{H} + \hat{S}\cdot\mathbf{A}\cdot\hat{I} + \hat{I}\cdot\mathbf{P}\cdot\hat{I} - g_n\beta_n\hat{H}\cdot\hat{I}$$

Here, **g**, **A**, and **P** are tensors describing the electronic Zeeman interaction, the magnetic hyperfine interaction, and the quadrupole interaction, respectively. A computer program that calculates the ^{57}Fe Mössbauer spectrum of a paramagnetic polycrystalline sample employing the above spin Hamiltonian is available.[16] The eigenvalues and the eigenvectors of the nuclear states calculated with the above equation generally depend on the orientation of the molecule relative to the external magnetic field $\hat{H}$. The transition probabilities between these states depend on the direction of the γ-ray with respect to both the molecule and the external field.

Simulation of a Mössbauer spectrum with parameters characterizing both the principal component of the electric field gradient and the **g** tensor in their principal axis systems yields a value for the effective magnetic field at the ^{57}Fe nucleus. This effective field can be defined as the vector sum of the externally applied magnetic field ($\hat{H}_{ext}$) and the internal magnetic field ($\hat{H}_{int}$), since for large fields

$$\hat{I}\cdot\mathbf{A}\cdot\langle\hat{S}\rangle - g_n\beta_n\hat{H}_{ext}\cdot\hat{I} = -g_n\beta_n\hat{H}_{eff}\cdot\hat{I}$$

or simply

$$\hat{H}_{eff} = \hat{H}_{ext} + \hat{H}_{int}$$

where

$$\hat{H}_{eff} = \hat{H}_{ext} - \mathbf{A}\cdot\langle\hat{S}\rangle/g_n\beta_n$$

The internal field is comprised of contributions from three sources:

$$\hat{H}_{int} = \hat{H}_L + \hat{H}_d + \hat{H}_c$$

Frequently the most significant is the Fermi contact term, $\hat{H}_c$, an isotropic interaction which results from unpaired spin density at the ^{57}Fe nucleus. In ionic iron complexes where the unpaired spin density is produced by 3d-polarization effects on the internal s shells, the value of $\hat{H}_c$ at low temperatures is of the order of -110 kG for each unpaired 3d electron.[17] Both $\hat{H}_L$ and $\hat{H}_d$ (the orbital and dipolar fields, respectively) normally contribute anisotropically to the hyperfine field. $\hat{H}_L$ arises from the orbital angular momentum of the electrons, while $\hat{H}_d$ results from the dipolar interaction between the spin magnetic moment of the ^{57}Fe nucleus and that of each unpaired electron.

From the above qualitative discussion it is clear that the Mössbauer technique can be used to gain some insight about the nature of the molecular orbital in which the single unpaired electron resides in a mixed-valence biferrocene. If this molecular orbital is largely a fulvalenide ligand orbital with little iron 3d-orbital contribution, the value of $\hat{H}_{int}$ will be negligible and $\hat{H}_{eff}$ will be approximately equal to $\hat{H}_{ext}$. However, even if the unpaired electron resides in an orbital which has appreciable d-orbital contribution, it is possible that the always negative Fermi contact term $\hat{H}_c$ could be offset by equal and opposite sign contributions from $\hat{H}_L$ and/or $\hat{H}_d$. It must be pointed out that it is frequently difficult to decide upon a breakdown of the experimentally determined $\hat{H}_{int}$ into the three types of contributions. For example, the experimental value of $\hat{H}_{int}$ for $K_3Fe(CN)_6$ is +255 kG.[18-20] Lang and Dale[21] employed a crystal field model to apportion the experimental $\hat{H}_{int}$. The principal components of $\hat{H}_c$, $\hat{H}_L$, and $\hat{H}_d$ were calculated to be -45.3, 357.3, and -37.8 kG, respectively, to give a net zth component of 274.2 kG. This breakdown, however, is somewhat controversial.

There is one other potential problem in the evaluation of $\hat{H}_{int}$ at a particular ^{57}Fe site in a compound. It is well-known that spin–spin and spin–lattice relaxation can have dramatic effects on the appearance of Mössbauer spectra. Either type of relaxation leads to an electronic spin–flip which results in a reversal of the magnetic hyperfine field $\hat{H}_{int}$. If the relaxation rate is slow on the Mössbauer time scale (rate less than approximately 10^6 s^{-1}), then the internal hyperfine field will appear to be fixed during the time for the Mössbauer transitions. On the other hand, if the relaxation rate is fast on the Mössbauer time scale (greater than approximately 10^9 s^{-1}), then the internal hyperfine field $\hat{H}_{int}$ due to the unpaired electrons will be reversing rapidly during the time of the Mössbauer transition. In this case the magnetic field at the nucleus due to the unpaired electrons will be greatly reduced (essentially zero), and $\hat{H}_{eff}$ will appear to be equal to $\hat{H}_{ext}$. In general, for paramagnets at temperatures less than 70 K and applied magnetic fields greater than 30 kG there will be an appreciable difference in the Boltzmann population of spin-up and spin-down molecules (electronic Zeeman interaction greater than the thermal energy) and, as a consequence, the net $\hat{H}_{int}$ at the nucleus will not average to zero when the electronic relaxation rate is fast on the Mössbauer time scale. For example, a $g = 2$, $S = {}^1/_2$ species in a 60-kG field at 5 K will have 20% of the molecules with electrons in the $M_s = +{}^1/_2$ level and 80% in the $M_s = -{}^1/_2$ level.

Intermediate possibilities, of course, also exist where the electron spins are relaxing at a rate comparable with that of the nuclear Larmor precession frequency. Spectra resulting from this situation are quite complex in their analysis and require the use of a time-dependent Hamiltonian.

Results and Discussion

Ferrocene and Substituted Ferrocenium Monomers. The Mössbauer spectrum for a localized (i.e., one Fe(II) and one Fe(III) doublet in zero field) mixed-valence biferrocene in high magnetic field would be naively expected to consist of a superposition of the spectrum for the ferrocene half and the spectrum for the ferrocenium half. It is appropriate then to discuss our Mössbauer results for ferrocene and a number of monomeric substituted ferrocenium cations before we discuss our results for the binuclear mixed-valence species.

The spectrum for a sample of ferrocene at 10 K in a 60-kG field is illustrated in Figure 1. This is the characteristic "doublet–triplet" pattern seen for a diamagnetic material with η close to zero. The spectrum was simulated with $\hat{H}_{eff} = \hat{H}_{ext} =$ 59.7 kG, $\Delta E_Q = 2.38$ mm/s, $V_{zz} > 0$, $\eta = 0$, and $\Gamma_{1/2} = 0.14$ mm/s. This is in good agreement with previous analyses[22] of the Mössbauer spectrum of magnetically perturbed ferrocene. Since

(15) Gütlich, P.; Link, R.; Trautwein, A. "Mössbauer Spectroscopy and Transition Metal Chemistry"; Springer-Verlag: New York, 1978.
(16) Münck, E.; Groves, J. L.; Tumolillo, T. A.; Debrunner, P. G. *Comput. Phys. Commun.* **1973**, *5*, 225.
(17) Greenwood, N. N.; Gibb, T. C. "Mössbauer Spectroscopy"; Chapman and Hall Ltd: London, 1971; p 103.
(18) Oosterhuis, W. T.; Lang, G. *Phys. Rev.* **1969**, *178*, 439.
(19) Ono, K.; Shinohara, M.; Ito, A.; Sakai, N.; Suenaga, M. *Phys. Rev. Lett.* **1970**, *24*, 770.
(20) Chappert, J.; Sawicka, B.; Sawicki, J. *Phys. Status Solidi B* **1975**, *72*, K139.
(21) Lang, G.; Dale, B. W. *J. Phys. C* **1973**, *6*, L80.
(22) Collins, R. L. *J. Chem. Phys.* **1965**, *42*, 1072.

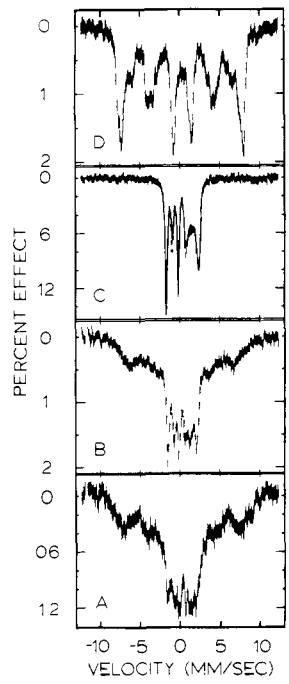

Figure 1. 5 K, 60-kG Mössbauer spectra for (A) compound VI and (B) compound VII; the 10 K, 60-kG spectra for (C) ferrocene, and (D) ferrocenium hexafluorophosphate.

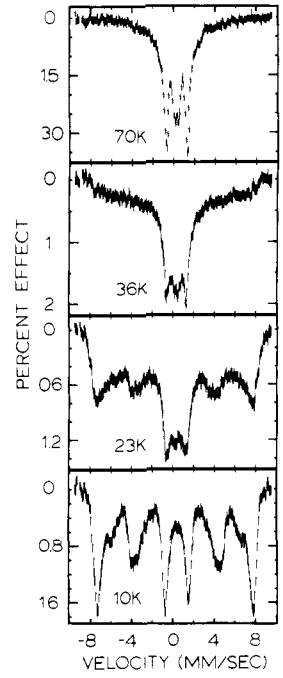

Figure 2. Variable-temperature 60-kG Mössbauer spectra of ferrocenium hexafluorophosphate.

ferrocene is diamagnetic and ΔE_Q is nearly temperature independent, no temperature dependence of this "doublet–triplet" pattern is expected.

The 10 K, 60-kG spectrum for ferrocenium hexafluorophosphate in Figure 1 is significantly different from that of ferrocene, demonstrating the dramatic effects an unpaired electron can have on a magnetic field Mössbauer spectrum. In this case, $\hat{H}_{eff}$ felt by the ^{57}Fe nucleus results primarily from the field set up by the unpaired electron of this $S = {}^1/_2$ iron(III) complex. It is clear that the ferrocenium PF_6^- spectrum results from a species with a relatively slow electronic relaxation, ΔE_Q close to zero, and appreciable **g**- and **A**-tensor anisotropy. The principal component of the effective magnetic field at the nucleus is ~478 kG (calculated from the energy difference of the two outermost peaks using the Zeeman Hamiltonian), a field much larger than the isotropic 110-kG field which might be expected from the Fermi contact contribution alone. Frankel et al.[14] reported a 60-kG spectrum of ferrocenium hexafluorophosphate measured at 4.2 K. They simulated their spectrum with a computer program[23] (which does not parameterize the **g**- and **A**-tensors) to obtain ΔE_Q = 0.20 mm/s, $\eta = 0$, and $\hat{H}_{eff}$ = 474 kG while noting absorptions of the $\Delta M_I = 0$ transitions indicative of "an anisotropic **g** tensor". Furthermore, with measurements at various external fields up to 80 kG they found that $\hat{H}_{int} = +414$ kG.

It is quite reasonable that the iron nucleus in the ferrocenium ion has a large orbital contribution ($\hat{H}_L$) to the internal hyperfine field, since it is well-known that there is appreciable orbital angular momentum in the ground state of the complex. The electronic ground state of the D_{5d}-symmetry ferrocenium ion is a Kramers doublet resulting from the effects of spin–orbit interaction and low-symmetry crystal fields upon a $^2E_{2g}$ state which arises from the $a_{1g}{}^2e_{2g}{}^3$ configuration.[24] The a_{1g} and e_{2g} one-electron orbitals are dominantly d-orbital in character: $a_{1g}(d_{z^2})$ and $e_{2g}(d_{x^2-y^2}, d_{xy})$.

Figure 2 illustrates the temperature dependence of the 60-kG spectrum of ferrocenium hexafluorophosphate. The strong temperature dependence of the effective field at the ^{57}Fe nucleus as evidenced by the broadening and collapse of the outer peaks reflects an increase in the electron spin relaxation rate with increasing temperature. By 70 K the spectrum has collapsed to a four-line pattern (roughly 3:1:1:3 relative intensities) with $\hat{H}_{eff} = \hat{H}_{ext} = 60$ kG. At this temperature the electronic relaxation is fast on the Mössbauer time scale and the M_s levels are nearly equally populated; consequently, $\hat{H}_{int}$ is nearly averaged to zero.

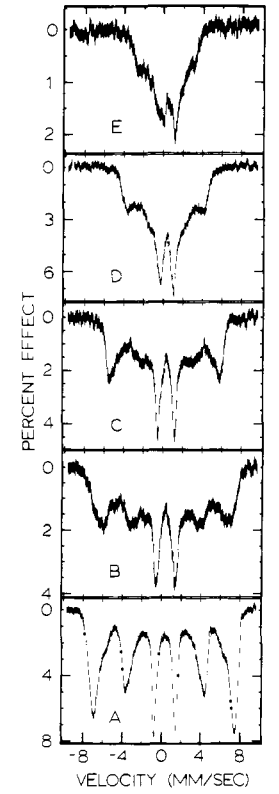

Figure 3. 5 K, 55-kG Mössbauer spectra for (A) ferrocenium hexafluorophosphate; (B) methylferrocenium hexafluorophosphate (II); (C) decamethylferrocenium hexafluorophosphate (III); (D) 1,1′-dimethylferrocenium hexafluorophosphate (IV); (E) 1,1′-trimethyleneferrocenium hexafluorophosphate (V).

It is important to understand whether the above electronic relaxation behavior observed for ferrocenium hexafluorophosphate is characteristic of all monomeric substituted ferrocenium cations.

(23) Gabriel, J. R.; Ruby, S. L. *Nucl. Instrum. Methods* **1965**, *36*, 23. Collins, R. L.; Travis, J. C. *Mössbauer Eff. Methodol.* **1967**, *3*, 123.
(24) Duggan, D. M.; Hendrickson, D. N. *Inorg. Chem.* **1975**, *14*, 955. Hendrickson, D. N.; Sohn, Y. S.; Gray, H. B. *Ibid.* **1971**, *10*, 1559.

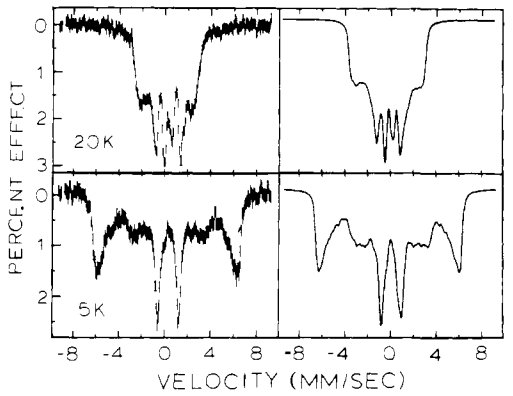

Figure 4. 5 and 20 K Mössbauer spectra of decamethylferrocenium hexafluorophosphate (III) in a 60-kG field. The two panels on the left show the experimental spectra, whereas the two right panels are the computer-simulated spectra obtained by employing the $S = {}^1/_2$ spin Hamiltonian program. Fast electronic relaxation is assumed (see text for parameters).

Mössbauer spectra were collected for the PF_6^- salts of the four substituted ferrocenium cations II–V at 5 K in a 55-kG field.

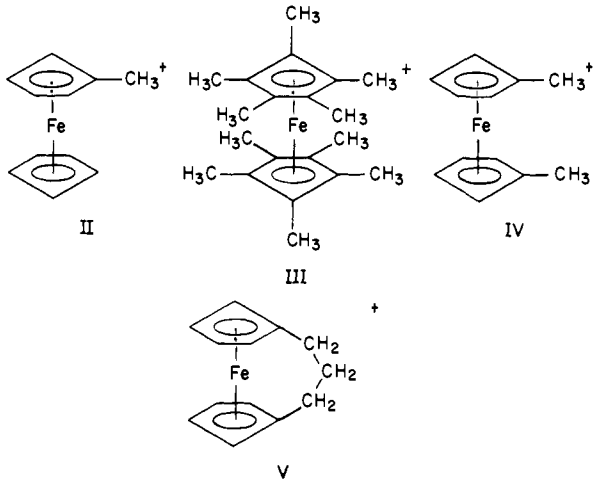

Figure 3 shows that a wide range of effective fields at the ^{57}Fe nucleus can be encountered for these monomeric ferrocenium cations. There are a number of possible explanations for this range of effective field values. The most likely possibility is that the electron spin relaxation rate (spin–lattice and/or spin–spin) varies across the series, averaging the internal field to a different value for each sample. It is interesting that, while the 5 K, 55-kG spectrum for ferrocenium PF_6^- is characteristic of a *slow* electronic relaxation rate, the 5 K, 55-kG spectrum for the decamethylferrocenium ion appears to be characterized by a *fast* electronic relaxation rate. Figure 4 shows the spectrum of species III both at 5 and 20 K in a 60-kG field. Theoretical simulations using $g_{xx} = 1.35$, $g_{yy} = 1.35$, $g_{zz} = 4.43$, $\Delta E_Q = 0.341$ mm/s, $A_{xx} = -110$ kG, $A_{yy} = -110$ kG, and $A_{zz} = +700$ kG are also shown for these two spectra where *fast electronic relaxation is assumed.* It can be seen that the experimental spectra bear a close resemblance to these simulated spectra. It should be noted that the 5 K, 60-kG spectrum for species III is a Boltzmann weighted average of spectra for $M_s = -{}^1/_2$ and $M_s = +{}^1/_2$ electrons, where there are more $M_s = -{}^1/_2$ electrons at this temperature. It is somewhat surprising, but quite evident, that fast- and intermediate-relaxation spectra are seen for these ferrocenium salts even at 5 K.

It is also possible that the internal fields vary across the above series of substituted ferrocenium cations because of different values and/or alignments (vectorial addition) of $\hat{H}_L$, $\hat{H}_d$, and $\hat{H}_c$. The amount of orbital angular momentum in the ground state does vary somewhat across the above series of ferrocenium cations. This is substantiated by the variation in g-values seen for some of these PF_6^- salts.[24] The PF_6^- salt of cation III has a **g**-tensor anisotropy with $g_\parallel = 4.43$ and $g_\perp = 1.35$ not unlike that of the unsubstituted ferrocenium ion. The PF_6^- salt of cation IV has $g_\parallel = 4.00$ and $g_\perp = 1.92$. A maximum in low-symmetry distortion (minimum in orbital angular momentum) is found for the PF_6^- salt of cation V with $g_\parallel = 3.86$ and $g_\perp = 1.81$. Certainly this variation in orbital angular momentum across the series would also lead to a variation in spin–lattice relaxation.

It should be pointed out that there could be a potential problem associated with the extrapolation of low magnetic field (3 kG) g-value measurements to the high-field (60 kG) region employed in the Mössbauer work. The high magnetic field could produce admixtures of excited states into the ground state up and beyond what is present at low fields. As a consequence, internal fields and relaxation rates could be different at low and high magnetic fields. However, our simulations (vide supra) of Mössbauer spectra of two monomeric ferrocenium salts in high magnetic fields did succeed even though we employed g-values determined in low fields.

The above results indicate that several factors can influence the appearance of the Mössbauer spectrum of a magnetically perturbed ferrocenium cation, substituted or not. Each iron(III) metallocene studied gives a unique and uniquely temperature-dependent magnetic Mössbauer pattern, possibly because the electron spin can be relaxing slow, fast, or at an intermediate rate relative to the nuclear Larmor precession frequency. It is clear that in order to determine accurately $\hat{H}_{int}$ at the ^{57}Fe site in a mixed-valence biferrocenium, it is necessary to be sure that the Mössbauer spectrum is not affected by spin–lattice or spin relaxation effects. Although an examination of the temperature dependence of the spectrum could prove to be useful, each of the spin–lattice relaxation mechanisms can have different temperature and magnetic field dependencies.[25] Clearly, the view that the Mössbauer spectrum for a localized mixed-valence biferrocene in a high magnetic field will consist of a superposition of a ferrocene signal and a ferrocenium hexafluorophosphate signal is naive.

Mössbauer-Localized Mixed-Valence Biferrocenes. By all accounts the mixed-valence compound VI is a very localized (i.e., class I) species. The single-crystal X-ray structure[26] of this

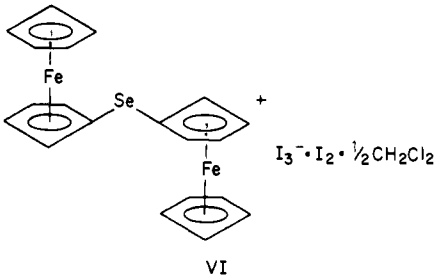

compound shows that the structure as a whole can be described in terms of cationic and anionic layers; the anionic layer is composed of zigzag chains of triiodide anions and iodine molecules. The mixed-valence selenium-bridged biferrocene cation assumes a gauche conformation intermediate between the cisoid and transoid conformations. The intramolecular Fe–Fe distance is 6.058 (2) Å and, as indicated by the centroid-to-centroid ring distances, the two $Fe(\eta^5\text{-}C_5H_5)(\eta^5\text{-}C_5H_4)$ moieties are structurally different. One is an iron(II) metallocene, and the other an iron(III) metallocene. In agreement with this, two quadrupole-split doublets are seen in the zero-field Mössbauer spectrum. In addition, no intervalence-transfer electronic absorption band is seen in the near-IR for compound VI. Compound VII is also a relatively localized mixed-valence biferrocene, where one ferrocenyl moiety is substituted by an acetyl group. Compound VII also gives a zero-field Mössbauer spectrum with two quadrupole-split doublets.[26]

(25) Stapleton, H. J. *Magn. Reson. Rev.* **1971**, *1*, 65. Stevens, K. W. H. *Rep. Prog. Phys.* **1967**, *30*, 189.
(26) Kramer, J. A.; Herbstein, F. H.; Hendrickson, D. N. *J. Am. Chem. Soc.* **1980**, *102*, 2293.

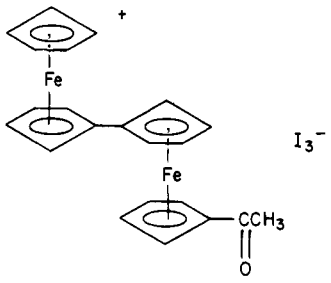

VII

Mössbauer spectra were run for compounds VI and VII at 5 K in a 60-kG field, as illustrated in Figure 1. It can be seen that these two 60-kG spectra are each essentially a superposition of a ferrocene and a ferrocenium 60-kG spectrum. In each case the ferrocenium-type spectral features are quite broad compared to those seen in the ferrocenium PF_6^- 60-kG, 10 K spectrum. Furthermore, the two outer peaks in the ferrocenium hexafluorophosphate spectrum appear at larger velocities than the corresponding peaks in the spectra of compounds VI and VII. Relaxation effects are evident in the 5 K, 60-kG spectra of compounds VI and VII.

Compound VIII is another well-characterized localized mixed-valence ferrocene. Single-crystal X-ray results[27] show that

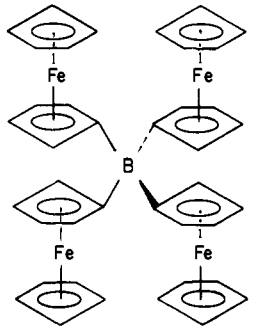

VIII

of the four metallocene units one is ferrocenium-like and the other three are ferrocene-like. Two quadrupole-split doublets, one for the iron(II) with ΔE_Q = 2.31 mm/s and the other for the iron(III) with ΔE_Q = 0.15 mm/s, are seen in the zero-field spectrum for this compound at 5 K. The 55-kG, 5 K Mössbauer spectrum in Figure 5 is, however, quite different from those seen above for complexes VI and VII. Although the ferrocene-like "doublet–triplet" signal is clearly visible, the ferrocenium-like signal can only partially be seen in the form of the weak features at +3.00 and −3.00 mm/s. It appears that the effective field has collapsed in compound VIII due to fast electron spin relaxation, as was seen for several of the substituted ferrocenium cations.

The PF_6^- salt of the mixed-valence biferrocene cation in a 60-kG field was studied previously with the Mössbauer technique by Frankel et al.[14] They used a computer program which does not parameterize the hyperfine interaction[23] to simulate their 4.2 K, 60-kG spectrum and concluded that they could identify the peaks for the two signals present. For the iron(II) signal they obtained from their simulation ΔE_Q = 1.85 mm/s, $V_{zz} > 0$, η = 0.9, and $\hat{H}_{eff}$ = 58 kG. For the iron(III) signal they obtained ΔE_Q = 0.48 mm/s, $V_{zz} > 0$, η = 0.9, and $\hat{H}_{eff}$ = 138 kG. The reduced effective field (138 kG vs. 474 kG for the ferrocenium ion) seen for the iron(III) part of the biferrocene cation led Frankel et al. to conclude that the unpaired electron is in a predominantly ligand-based orbital and that their results are not consistent with the view that the mixed-valence biferrocenium cation consists of ferrocene-like iron(II) and ferrocenium-like iron(III) moieties. These conclusions seem to contradict the EPR results for mixed-valence biferrocene salts, where $g_\parallel \simeq 3.5$ and $g_\perp \simeq 1.9$.[3] This large **g**-tensor anisotropy does *not* seem at all possible for an organic radical.

(27) Cowan, D. O.; Shu, P.; Hedberg, F. L.; Rossi, M.; Kistenmacher, T. J. *J. Am. Chem. Soc.* **1979**, *101*, 1304.

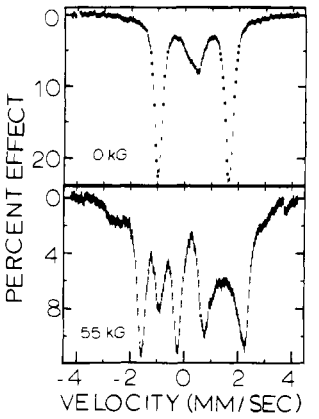

Figure 5. 5 K Mössbauer spectra of compound VIII in zero field and in a 55-kG external field.

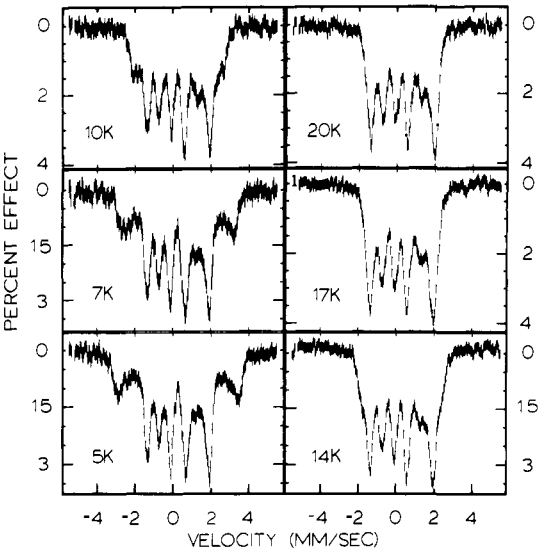

Figure 6. Variable-temperature 55-kG Mössbauer spectra of biferrocenium triiodide, compound IX.

We were thus particularly motivated to collect Mössbauer data for the triiodide salt of the same mixed-valence biferrocene cation (compound IX) in a high magnetic field. There is no question

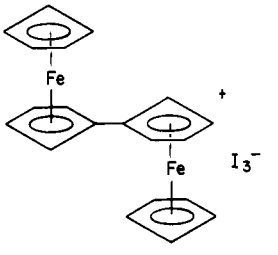

IX

that the mixed-valence biferrocene cation in compound IX is localized on the Mössbauer time scale Two quadrupole-split doublets are seen in the *zero-field* spectrum for this compound at 5 K. One doublet is characterized by ΔE_Q = 2.1 mm/s and the other by ΔE_Q = 0.40 mm/s.

The 55-kG Mössbauer spectrum for compound IX was run at several temperatures, as can bee seen in Figure 6. At 5 K distinct ferrocene-like iron(II) and ferrocenium-like iron(III) patterns are evident; only two of the broad iron(III) signals are well resolved (at ~−3 mm/s and ~+3.2 mm/s). As the temperature of the sample is increased, it becomes increasingly difficult to identify distinct ferrocene-like and ferrocenium-like patterns. This dif-

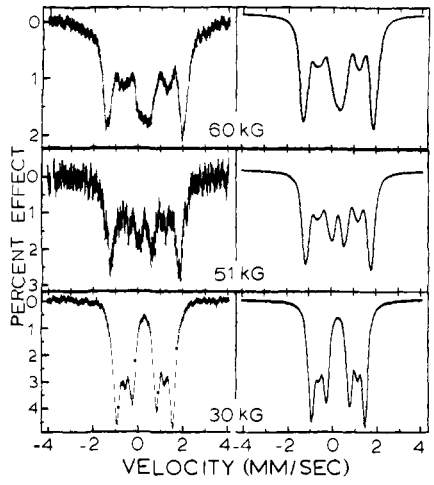

Figure 7. High-field 5 K Mössbauer spectra of bis(fulvalene)diiron triiodide, compound X, in magnetic fields of 30, 51, and 60 kG. The left panels show the experimental spectra, whereas the right panels illustrate the computer-simulated spectra obtained with the parameters given in the text.

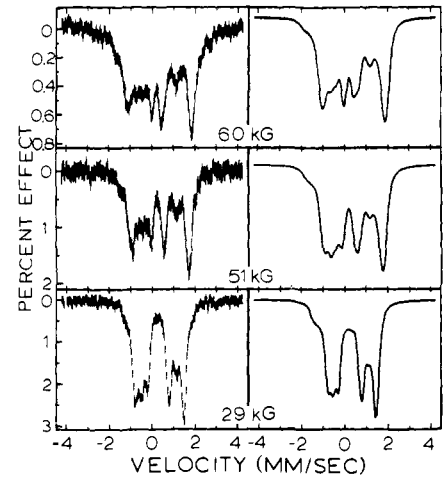

Figure 8. High-field 5 K Mössbauer spectra of [2,2]ferrocenophane-1,13-diyne triiodide–$^3/_4$ diiodine (compound XI) in magnetic fields of 29, 51, and 60 kG. The left panels show the experimental spectra, whereas the right panels illustrate the computer-simulated spectra obtained with the parameters given in the text.

ficulty obviously results from the collapse of the effective field associated with the iron(III) nucleus at higher temperatures, which is similar to what was seen for ferrocenium PF_6^- (see Figure 2). It is interesting to note that our spectrum for biferrocenium I_3^- at ~14 K is very similar to the spectrum reported by Frankel et al.[14] for biferrocenium PF_6^- at 4.2 K. In view of the temperature dependence that we see for the magnetic spectrum of biferrocenium I_3^- and the broadness of the iron(III) signals that are seen in the low-temperature spectrum, it seems very likely that the Mössbauer spectrum for either salt of the mixed-valence biferrocene cation is affected by an electronic relaxation rate that is either intermediate or fast on the Mössbauer time scale. If this is indeed the case, it is very difficult to simulate these Mössbauer spectra to assess $\hat{H}_{eff}$ for the iron(III) ion in the mixed-valence cation. The results reported in this paper for monomeric ferrocenium systems clearly indicate that fast electronic relaxation can occur in these iron(III) metallocenes even at liquid-helium temperatures and in a 60-kG applied field.

Mössbauer-Delocalized Mixed-Valence Biferrocenes. Two mixed-valence biferrocenes that persist as delocalized species at liquid-helium temperature were examined in high magnetic field with the Mössbauer technique. The following two solids each exhibit only one quadrupole-split doublet at ~5 K in zero applied field.

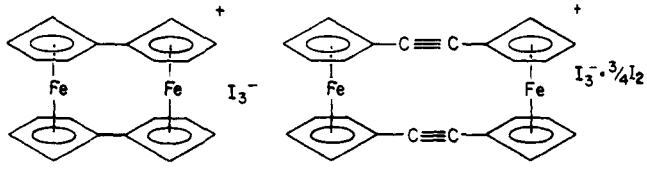

X XI

The mixed-valence bis(fulvalene)diiron cation in compound X is one of the more thoroughly studied mixed-valence biferrocenes. The iron ions in this species appear to be equivalent on the time scale of any physical technique.[3,4] Mössbauer spectra for compound X at 5 K and fields of 30, 51, and 60 kG are illustrated in Figure 7. Since there is only one type of iron ion present in this species and since the spectra do *not* appear to be affected by relaxation effects, we decided to try to simulate these three spectra. An X-band EPR spectrum was run for compound X at liquid-helium temperature to find a rhombic pattern with $g_z = 2.36$, $g_y = 1.99$, and $g_x = 1.91$. These g-values were employed together with $|\Delta E_Q| = 1.76$ mm/s to simulate the Mössbauer spectra for magnetically perturbed samples. The sign of the quadrupolar interaction, the asymmetry parameter η, and the components of the hyperfine tensor (A_{zz}, A_{yy}, and A_{xx}) were varied to find the best simulations of the three spectra taken at different fields. Furthermore, it was necessary without any additional data to assume that the **g**- and **A**-tensors are aligned. These simulated spectra are illustrated alongside the experimental spectra in Figure 7 and it can be seen that there is reasonable agreement. The parameters used to arrive at these simulations are ΔE_Q negative, $\eta = 0.8$, $A_{zz} = -6$ kG, $A_{yy} = -2$ kG, and $A_{xx} = -1$ kG. It is interesting that the hyperfine interaction (effective field at the nucleus) is found to be so small in this species. In view of the observed anisotropy in the **g**-tensor for this compound, it does *not* seem reasonable to conclude, however, that the mixed-valence bis(fulvalene)diiron cation is an organic radical with the single unpaired electron in an orbital that is largely fulvalenide in construction. It is more reasonable to conclude that either the various contributions ($\hat{H}_L$, $\hat{H}_d$, and $\hat{H}_c$) to $\hat{H}_{int}$ are canceling each other out, or the **g**-, **A**-, and **P**-tensors are *not* aligned. In fact, Hillman and Kvick[28] just reported the results of their X-ray structural work on the picrate salt of the mixed-valence bis(fulvalene)diiron cation. In this salt the mixed-valence cation is appreciably distorted with nonplanar fulvalenide ligands and a shorter Fe–Fe distance than in the neutral molecule. Indeed, it seems likely that the various tensors would be misaligned. Single-crystal EPR and ENDOR work is needed.

Figure 8 illustrates the Mössbauer data for compound XI obtained at 5 K in fields of 29, 51, and 60 kG. The X-band EPR spectrum of this compound at 5 K gave a rhombic signal with g-values of $g_z = 2.52$, $g_y = 1.97$, and $g_x = 1.88$, not unlike what is reported in the literature.[3] The sign of ΔE_Q, and magnitudes of η, A_{zz}, A_{xx}, and A_{yy} were varied to obtain the reasonable simulations illustrated in Figure 8. The final simulation parameters are: $\Delta E_Q = +1.62$ mm/s, $\eta = 0.85$, $A_{zz} = +8$ kG, $A_{yy} = -81$ kG, and $A_{xx} = -5$ kG. While it is clear that these parameters do not provide an exact simulation, extensive searches into parameter space have been conducted and the above parameters give the best simulated spectra. The conclusion drawn from these searches is that if **g**, **A**, and **P** are assumed to be aligned, then at least one of the components of the hyperfine tensor is large (i.e., on the order of 100 kG) and negative. Assuming that the **A**-tensor is symmetric (required only if the symmetry is orthorhombic or higher), then an average hyperfine interaction can be calculated where $A_{av} = (A_{zz}^2/3 + A_{yy}^2/3 + A_{xx}^2/3)^{1/2}$ and is equal to 47 kG. This internal field is somewhat less than the Fermi contact field expected for one unpaired electron interacting equivalently with two iron ions, which gives $\hat{H}_{int} = 55$ kG. Until structural work is done on this species it is not possible to know whether the **g**- and **A**-tensors could be misaligned.

(28) Hillman, M.; Kvick, Å. *Organometallics* **1983**, *2*, 1780.

Conclusions

The Mössbauer spectra for mononuclear substituted ferrocenium species in large applied magnetic fields have been shown to have a variety of appearances. It was concluded that differences in the rates of electronic relaxation from one substituted ferrocenium to another lead to the variability in appearance of Mössbauer spectra of ferrocenium in salts in high magnetic fields. Direct evidence was found for this from variable-temperature Mössbauer studies of ferrocenium hexafluorophosphate and decamethylferrocenium hexafluorophosphate, both in a 60-kG field. On the Mössbauer time scale, slow electronic relaxation is present in ferrocenium hexafluorophosphate, whereas fast electronic relaxation is present in the decamethylferrocenium salt. This latter fact was substantiated by computer simulation of Mössbauer spectra with a program developed from the $S = {}^1/_2$ spin Hamiltonian. It is clear, then, that any interpretation of the Mössbauer spectra of mixed-valence biferrocenes in high magnetic fields has to take into account the possibility of slow, fast, or intermediate electronic relaxation. In fact, in the case of two localized mixed-valence biferrocenes we did find that the Mössbauer spectra are superpositions of ferrocene and (unsubstituted) ferrocenium signals, where the ferrocenium signal reflects a relatively slow electronic relaxation. However, in the case of several other "Mössbauer-localized" mixed-valence biferrocenes the effective magnetic field at the Fe(III) nucleus was found to be considerably reduced compared to the 474 kG found for ferrocenium hexafluorophosphate. From a study of the temperature dependence of the spectra it was concluded that these reduced effective fields are most likely due to electronic relaxation that is either intermediate or fast on the Mössbauer time scale.

The 5 K, 60-kG Mössbauer spectra of two "Mössbauer-delocalized" biferrocenes were also simulated with the $S = {}^1/_2$ spin Hamiltonian computer program. With the assumption of aligned **g**- and **A**-tensors, it was found in one case that the iron hyperfine interaction is quite small, whereas in the other case the hyperfine interaction is approximately what would be expected for the Fermi contact interaction of one unpaired electron interacting equivalently with two iron nuclei.

Experimental Section

Mössbauer Spectroscopy. The ^{57}Fe Mössbauer spectra were obtained in vertical transmission geometry using a constant acceleration spectrometer. The source, which originally consisted of 50 mCi of ^{57}Co diffused into a 12-μm rhodium matrix, is connected to a Ranger Scientific Model VT-700 velocity transducer via a 4-ft-long $^1/_4$-in.-diameter stainless steel tube (later changed to a $^1/_4$-in. phenolic fiberglass rod to prevent high-frequency vibrations of the tube). Transverse motion of the tube is prevented with the use of a small stainless steel spring[29] located several inches from the source. This spring is coupled to the source, absorber, and transducer via three 49-in.-long $^1/_8$-in.-diameter stainless steel rods located concentrically about the $^1/_4$-in. tube.[30] At the far end of the rods (which are supported by spacers every 5 in.) is the absorber, located approximately 3 in. from the source. This entire assembly is placed inside a Janis Model 21-CNDT gas-flow cryostat equipped with a 60-kG superconducting magnet. A pair of aluminized Mylar windows, one at the bottom of the helium can and the other on the outside of the cryostat, are the only attenuators of the γ-rays. A shielded Reuter-Stokes proportional counter powered by an Ortec Model 456 high-voltage power supply is used to detect the γ-rays. An Ortec Model 142PC preamplifier and an Ortec Model 571 amplifier are used to amplify the signals before selecting only the 14.4-KeV pulses with an Ortec Model 550 single-channel analyzer. A Canberra series 30 multichannel analyzer (MCA), scanned over 512 channels every 0.205 s (4.88 Hz), receives the logic pulses from the single-channel analyzer. The MCA supplies a half-memory pulse for synchronization with the transducer. This signal is then integrated by the Ranger MS-700 spectrometer to provide the symmetric triangular waveform which drives the transducer.

After data collection is completed, the resulting mirror-image spectra are transferred to a Digital Corp. VAX 11/780 computer, where they are "folded" into a single 256-channel spectrum, effectively canceling their parabolic base lines.

Computer fittings of the ^{57}Fe Mössbauer data to Lorentzian lines were carried out with a modified version of a previously reported program.[31] The computer simulations of magnetic spectra with a $S = {}^1/_2$ spin Hamiltonian were carried out with a second computer program.[16]

Velocity calibrations were made by using a 99% pure 12.7-μm iron foil. Typical line widths for all three pairs of iron lines fell in the range 0.24–0.28 mm/s. Isomer shifts are reported with only the room-temperature correction for Fe in Rh applied. Due to experimental difficulties (the cooled source temperature varies with absorber temperature), a full correction was not attempted.

The Mössbauer sample cell consists of a pair of concentric Delrin plastic cups. This cell fits tightly into a larger cylindrical copper block which has a 45-Ω heater wire wound around the outer circumference. Temperature control is by means of a Lake Shore Cryotronics Model DTC-500-SP temperature controller. Sample temperature measurements are made with a calibrated Allen Bradley 560-Ω, $^1/_8$-W carbon resistor, mounted in the copper sample cell holder (estimated accuracy below 10 K is $\sim$1 K, for the region 10–30 K it is better than 2 K, and from 30 to 70 K the temperature is known within 3 K).

For magnetic field Mössbauer measurements, the superconducting solenoid is energized with a Sorenson SRL10-100 precision power supply in conjunction with an American Magnetics Model 400 programmer and Model 510 persistent current switch. The source was shielded from the field by two "bucking" coils and remained unsplit to 2 K. The applied field was calibrated by using a diamagnetic potassium ferrocyanide absorber and an axial Hall probe, Siemans Corp. No. RHY17. Reproducibility and accuracy of magnetic field measurements were found to be no better than $\pm$1.0 kG.

Sample Preparation. Samples of ferrocenium hexafluorophosphate and the PF_6^- salts of complexes II–V were prepared as reported previously.[24] Samples of the various mixed-valence biferrocenes were available from previous studies.[3,5,26]

Acknowledgment. We are grateful for support from NIH Grant HL 13652. Partial funding for the Mössbauer equipment came from NSF grant CHE 78-20727, combined with equal funding from our chemistry department and the Research Board of the University of Illinois. We are thankful to Professor Dwaine Cowan for a sample of complex VIII and to Dr. Manny Hillman for a preprint of ref 28. We are particularly indebted to Professor Peter Debrunner not only for a copy of the $S = {}^1/_2$ spin Hamiltonian computer simulation program but also for several useful discussions.

Registry No. II, 92078-16-5; III, 54182-44-4; IV, 51512-99-3; V, 54191-91-2; VI, 74204-54-9; VII, 74779-55-8; VIII, 69930-51-4; IX, 39470-17-2; X, 39333-89-6; XI, 74779-53-6; ferrocene, 102-54-5; ferrocenium hexafluorophosphate, 11077-24-0.

(29) A computer program to generate these springs is available, see: Federer, W. D. Ph.D. Thesis, University of Illinois, 1984.

(30) Kalvius, M. *Mössbauer Eff. Methodol.* **1965**, *1*, 163.

(31) Chrisman, B. L.; Tumolillo, T. A. *Comput. Phys. Commun.* **1971**, *2*, 322.